IEEE Photonics Journal
An IEEE Photonics Society Publication

Open Access

High Power (>27 W) Semiconductor Disk Laser Based on Pre-Metalized Diamond Heat-Spreader

Volume 11, Number 2, April 2019

Guan-Yu Hou
Shi-Li Shu
Jian Feng
Andreas Popp
Berthold Schmidt
Huan-Yu Lu
Li-Jie Wang
Si-Cong Tian
Cun-Zhu Tong
Li-Jun Wang

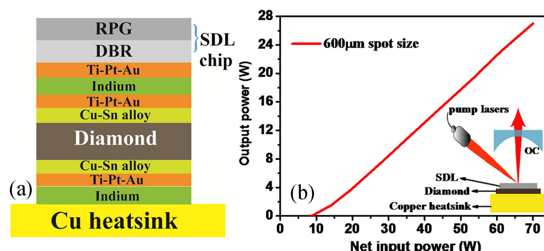

DOI: 10.1109/JPHOT.2019.2908876

IEEE photonics SOCIETY
IEEE

High Power (>27 W) Semiconductor Disk Laser Based on Pre-Metalized Diamond Heat-Spreader

Guan-Yu Hou ,[1,2] Shi-Li Shu,[1] Jian Feng,[1,2] Andreas Popp,[3]
Berthold Schmidt ,[3] Huan-Yu Lu,[1,2] Li-Jie Wang,[1] Si-Cong Tian,[1]
Cun-Zhu Tong ,[1] and Li-Jun Wang[1]

[1]State Key Laboratory of Luminescence and Applications, Changchun Institute of Optics, Fine Mechanics and Physics, Chinese Academy of Sciences, Changchun 130033, China
[2]Center of Materials Science and Optoelectronics Engineering, University of Chinese Academy of Sciences, Beijing 100049, China
[3]TRUMPF GmbH+Co.KG, Ditzingen 71254, Germany

DOI:10.1109/JPHOT.2019.2908876
This work is licensed under a Creative Commons Attribution 3.0 License. For more information, see https://creativecommons.org/licenses/by/3.0/

Manuscript received February 27, 2019; revised March 25, 2019; accepted March 28, 2019. Date of publication April 11, 2019; date of current version April 17, 2019. This work was supported in part by the TRUMPF GmbH and in part by the National Natural Science Foundation of China under Grants 61790584, 61761136009, and 61774153. Corresponding author: Cun-Zhu Tong (e-mail: tongcz@ciomp.ac.cn).

Abstract: High power semiconductor disk lasers (SDLs) were demonstrated based on the thermal management using pre-metalized diamond heat-spreader. The processing of pre-metallization using Cu-Sn alloy was developed. The resultant and influence of pre-metallization on the thermal performance of SDLs were investigated. It was found that the pre-metalized diamond heat-spreader was able to improve effectively not only the thermal resistance but also the bonding quality. 38% decrease on the thermal resistance of SDL was realized. The CW power exceeding 27 W, limited by the available pump power, was demonstrated.

Index Terms: High power, thermal management, metallization, semiconductor disk laser, vertical external-cavity surface-emitting laser (VECSEL).

1. Introduction

Semiconductor disk lasers (SDLs) [1]–[3], also known as optical pumped semiconductor vertical external cavity surface-emitting lasers (OPS-VECSELs) [4]–[7], are very attractive for high-power and high beam quality operation. This type laser is quite similar with the diode-pumped solid-state lasers but the gain medium is semiconductor quantum-wells (QWs) [3]–[7], which takes the advantages of semiconductor lasers, such as the versatile wavelength, wide-pumping bandwidth, and efficient pump absorption. Moreover, compared with conventional electrical-driven semiconductor diode lasers, SDL has no electrical injection and does not require the doping in the epitaxial growth, which simplifies the growth and reduces the optical loss resulted by the free carrier absorption.

However, the power scaling of SDL is quite challenging because of the high optical pump density of multi-kW/cm^2 and high thermal resistance of periodic structure and substrate [8], [9]. The heat dissipation is still one of the main reasons limited the output power of SDL in spite of the improved power in the last decades [10], [11]. Overheating leads to the thermalization of carriers in QWs and the misalignment between the QW positions and the anti-nodes of resonant periodic gain

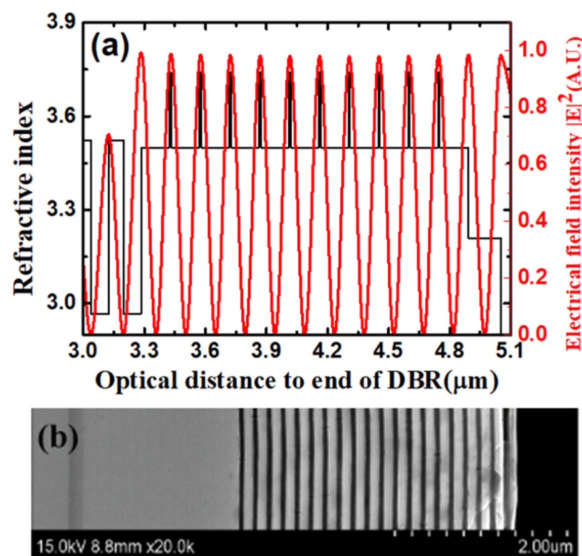

Fig. 1. (a) Refractive index profile and the standing wave distribution of designed SDL. (b) SEM image of the grown SDL structure.

structure (RPG) due to the different shift rates of material gain peak and the antinode of the laser field. In addition, the increased temperature degrades the gain and aggravates the non-radiative recombination [11]–[13]. One of the useful approaches to solve this issue is to solder the SDL on the diamond heat-spreader, which is generally achieved via solid-liquid interdiffusion of indium [10], [14], and the diamond heat-spreader is covered by Ti/Pt/Au firstly. The role of the Au layer is bonding with indium during the diffusion process, and the Pt layer provides a diffusion barrier between Ti and Au, which is necessary to strengthen the Ti-diamond bonding. Unfortunately, it was found that Pt tended to diffuse to the surface and condense during electron beam evaporation, which deteriorated seriously the bonding quality [15] and hence increased the thermal resistance of SDL.

In this paper, we proposed a pre-metallization method of diamond and demonstrated the high power continuous wave (CW) operation of SDL based on the pre-metalized diamond heat-spreader. The composition and resultant of pre-metallization by Cu-Sn alloy were analyzed. The thermal resistances of SDL with and without pre-metallization were estimated. The influence of the pre-metalized diamond heat-spreader and pump spot size on the heat dissipation and output power of SDLs were investigated.

2. Design and Experimental Setup

The SDL was designed with ten 8 nm InGaAs QWs embedded in the RPG structure with the optimized anti-nodes positions of the standing wave in the optical cavity to ensure a low threshold and homogeneous gain [16]. Fig. 1(a) shows the refractive index profile and the standing wave pattern of designed SDL. The distributed Bragg reflector (DBR) is 20 pairs AlAs/GaAs. The SDL structure was grown by metal-organic vapor phase epitaxy (MOVPE) on a GaAs substrate in a reverse order, which allows the removing of the substrate to reduce the thermal resistance. Fig. 1(b) illustrates the whole structure measured by scanning electron microscope (SEM). From the bottom to up, the structure consists of a half wavelength InGaP window layer that prevents carriers from diffusing to the chip surface and non-radiative recombining there [17], and an RPG structure with the designed emission wavelength of 1030 nm. After that, it is 20 pairs AlAs/GaAs DBR. The InGaP window layer also served as an etch stop layer.

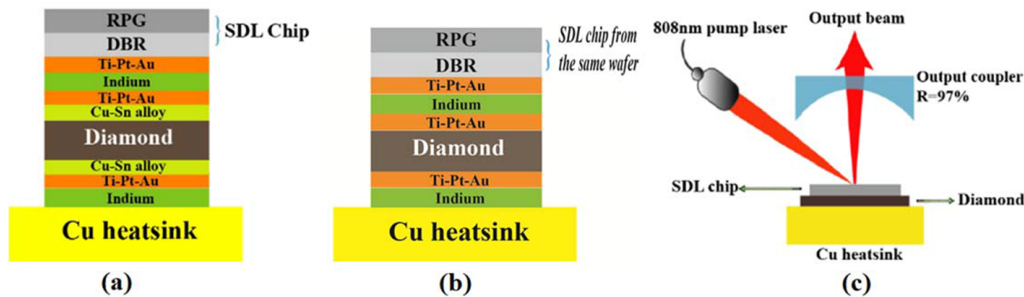

Fig. 2. Schematic diagram of SDL bonded on (a) pre-metalized diamond and (b) non-pre-metalized diamond. (c) The setup of pumping SDL.

Table 1
Material Compositions of the Cu-Sn Alloy (wt%)

Cu	Sn	Zn	Pb
82%-88%	5%-7%	5%-7%	2%-4%

The detailed packaging structures of SDL with and without pre-metallization processing of diamond are shown in Fig. 2(a) and (b), respectively. The disk chip was cleaved into 3 mm $\times$ 3 mm pieces and the Ti/Pt/Au layers were evaporated using electron beam evaporation on the DBR side of the SDL chip. The polycrystalline diamond was grown by chemical vapor deposition (CVD) and cut as the heat-spreader with dimensions of 5 mm $\times$ 5 mm $\times$ 1.2 mm. The pre-metallization of diamond was performed by depositing Cu-Sn alloy, whose compositions before deposition was shown in Table 1. It is alloy powder and over 82% is Cu. Sn element occupies 5%–7%. Before the pre-metallization, the diamond was cleaned by ultrasonic wave by dipping in acetone, methanol and isopropanol in sequence. After that, the diamond and the evaporation source of Cu-Sn alloy powder were put into the thermal evaporation coating machine. The diamond was heated up to 200 °C during the depositing, and the deposition rate was 0.6 nm–1.2 nm per minute. The thickness of the pre-metalized Cu-Sn layer on the diamond was 100 nm. After deposition of the pre-metalized Cu-Sn layer, the Ti/Pt/Au layers were grown with the thickness of 60 nm/60 nm/250 nm on both sides of diamond for the purpose of bonding with SDL chip and copper heatsink using indium. For the packaging without pre-metallization processing, the diamond was deposited directly with Ti/Pt/Au, just as shown in Fig. 2(b). In a final step, the GaAs substrate was removed by selective wet etching and the diamond was attached to a large copper heatsink mounted on thermoelectric cooler (TEC) using indium, which was performed in the reflow oven at 200 °C. Heat transferred by the TEC was removed by a water cooling system.

The experimental setup of SDL was shown in Fig. 2(c). In this linear cavity, an external mirror with a curvature radius of 100 mm and transmissivity of 3% was chosen as an output coupler (OC). The cavity length between the SDL chip and the external mirror was 60 mm. The chip was pumped using a fiber-coupled 808 nm diode laser with maximum power of 100 W. The pump beam was incident under a 45° angle and focused into 400 μm spot size on SDL surface by fiber optics. According to the curvature radius of OC and the distance to the chip, the diameter of TEM_{00} mode on the chip was calculated to be 254 μm from the equation in Ref. 2, which means this SDL operates at multi-modes if the pump spot diameter is larger than 254 μm.

3. Results and Discussion

Figure 3 shows the output power versus the net input power curves at the TEC temperature of 12 °C. The diameter of the pump spot is 400 μm. The SDL with pre-metalized diamond (solid circles) yielded a maximum output power of 24.5 W at the net input power of 70 W. The threshold

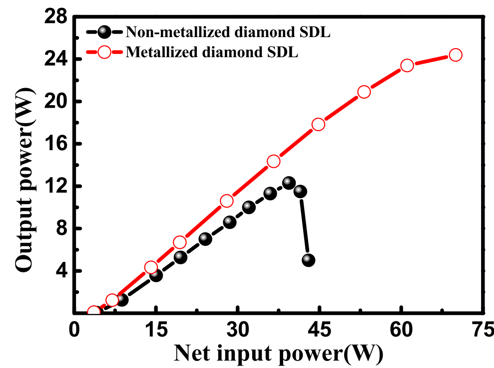

Fig. 3. Output power of SDLs bonded on diamond heat-spreader with (hollow circles) and without (filled circles) pre-metallization. The diameter of pump spot is 400 μm.

pump power is 3.64 W and the maximum optical-to-optical efficiency is 45%. The highest power of pump source is 100 W, and there is no anti-reflection coating on the SDL surface, which results in about 30% reflection loss of pump power. So the highest net input power is 70 W for this SDL. To compare the influence of pre-metallization processing of diamond on the output power of SDL, a SDL chip from the same wafer was bonded on non-pre-metalized diamond, whose structure is shown in Fig. 2(b). As can be seen in Fig. 3, the maximum emission power of the SDL bonded on non-pre-metalized diamond (filled circles) was only 12.3 W at a pump power of 39.4 W. The threshold pump power is 4.10 W. An evident thermal rollover happens at high pump power. Note that the fast drop of power after rollover is partly because the heat load exceeds the dissipation capacity of TEC and hence results in the temperature increase quickly. The power improvement shown in Fig. 3 can be benefit from the improvement of thermal resistance of pre-metalized diamond, or the other reasons, such as the detuning between the spectral position of gain maximum and the cavity/RPG resonance [18]. To go deeply insight the role of pre-metallization of diamond on the improvement of thermal management of SDL, the thermal resistance of these two SDL chips was investigated.

The thermal resistance (R_{th}) of SDL can be estimated according to the equation [19], [20]:

$$Rth = \frac{\Delta T}{\Delta Pd} = \frac{\Delta\lambda}{\Delta Pd}\bigg|Tcst \times \frac{\Delta T}{\Delta\lambda}\bigg|Pcst \tag{1}$$

where T is the heatsink temperature, P_d is the dissipated power which is net input power minus output power. λ is the emission wavelength. $\Delta\lambda/\Delta P_d$ should be obtained at the constant temperature, and $\Delta T/\Delta\lambda$ should be evaluated by the temperature dependent wavelength shifts at constant pump power. Fig. 4 shows the measured wavelength shifts versus pump power at the constant TEC temperature of 12 °C and versus temperature at constant pump power for SDL bonded on (a) non-pre-metalized and (b) pre-metalized diamond. To avoid the additional self-heating, the pump power is set at a little higher than the threshold power during the measurement of temperature dependent wavelength. From the linear fitting of Fig. 4(a), we can get the $\Delta\lambda/\Delta P_d = 0.5363 \pm 0.0103$ nm/W, $\Delta T/\Delta\lambda = 0.1632 \pm 0.0127$ K/nm, then the $R_{th} = 3.29 \pm 0.30$ K/W is obtained. As to the SDL bonded on pre-metalized diamond, the fitting results show that $\Delta\lambda/\Delta P_d = 0.2763 \pm 0.0028$ nm/W and $\Delta T/\Delta\lambda = 0.1358 \pm 0.0044$ K/nm from Fig. 4(b), the corresponding thermal resistance is $R_{th} = 2.03 \pm 0.08$ K/W. The error here is the fitting error. In other words, the thermal resistance of the packaging structure of SDL is reduced by 38% using the pre-metalized processing. The investigations on the stable conditions at thermal rollover [20] imply that the maximum temperature inside the gain region at rollover (T_{ro}) is independent on the heat sink temperature T_{Hs}, and $T_{ro} = T_{Hs} + R_{th}P_{d,ro}$, where $P_{d,ro}$ is the dissipated power at rollover. Hence, we can estimate the power improvement at rollover due to the decrease of thermal resistance. For SDL bonded on non-pre-metalized diamond, $P_{d,ro}$ is about 27.1 W from Fig. 3, and the heatsink temperature is 12 °C. So the

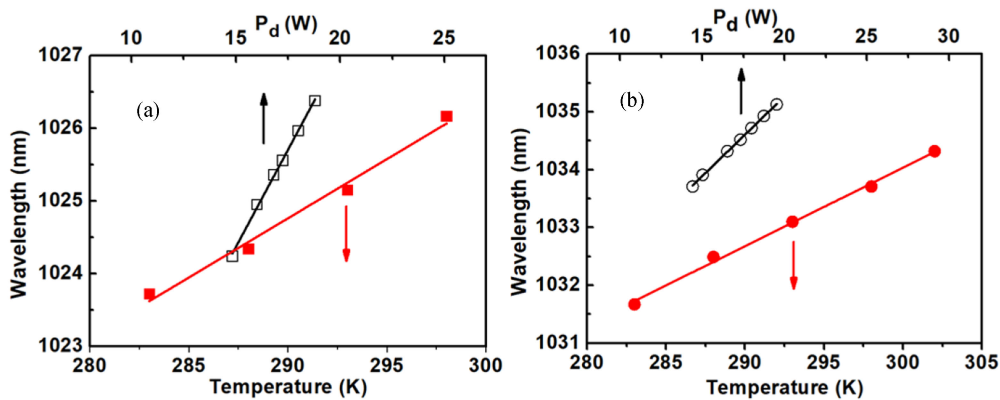

Fig. 4. Measured emission wavelength at different temperature (solid symbols) and dissipated power (hollow symbols) for SDLs bonded with (a) non-pre-metalized and (b) pre-metalized diamond.

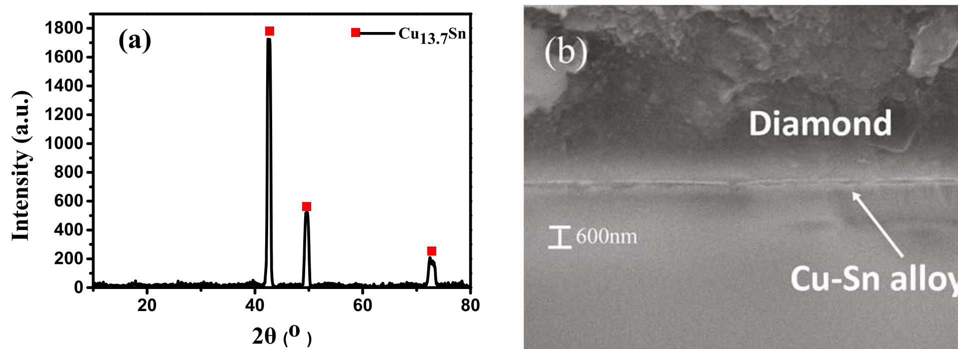

Fig. 5. (a) XRD result of deposited Cu-Sn alloy. (b) SEM image of the interface between diamond and Cu-Sn alloy.

estimated rollover temperature T_{ro} is about 101.2 °C. Then we can obtain the $P_{d,ro}$ of 43.9 W for SDL with $R_{th} = 2.03$ K/W. If it is only the improvement of thermal resistance and has no the changing of matching situation between the spectral position of gain maximum and the cavity/RPG resonance, the slope efficiency should be same as the power curve of SDL bonded on non-pre-metalized diamond. Then it can be estimated that the $P_{d,ro}$ of 43.9 W is able to increase the rollover power up to 21.1 W extrapolated from the power curve of SDL with non-pre-metalized diamond shown in Fig. 3, which is corresponding to a power improvement of 8.9 W. The realistic power improvement shown in Fig. 3 is 12.2 W. Hence, about 73% of the power improvement shown in Fig. 3 is due to the pre-metallization processing of diamond. The others might be resulted from the changing of matching between gain wavelength and cavity-mode wavelength. The SDL chips bonded on the pre-metalized and non-pre-metalized diamond are cut from the same wafer and adjacent position. The different lasing wavelength implies the different gain matching, which might be owing to the etching stop layer cannot be controlled sufficiently well during the removing of GaAs substrate. Any residual layers with thickness deviating from the half wavelength will make a cavity mode shift from the design value according to the transfer matrix theory.

The improved thermal resistance also benefits from the better quality of metallization and bonding, which was confirmed by the x-ray diffraction (XRD) and SEM measurement. Fig. 5(a) shows the XRD results of the metalized coating, which discloses that the effective component of the metalized coating layer is $Cu_{13.7}Sn$. Although the majority of deposited Cu-Sn alloy powder is Cu element, the realistic resultant is $Cu_{13.7}Sn$. The Sn element plays an important role in reducing the melting point and increasing the diffusivity of alloy [21]. Fig. 5(b) presents the SEM image of the interface between the diamond and Cu-Sn pre-metallization layer. The top part is the diamond. It can be

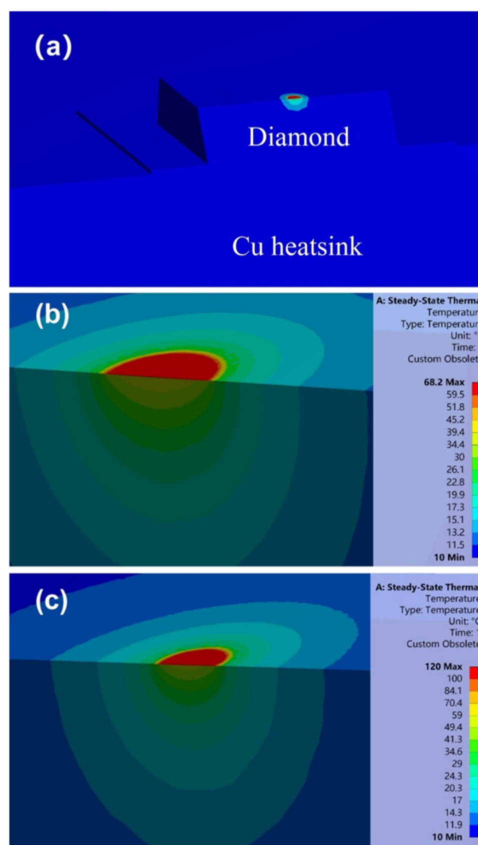

Fig. 6. (a) Schematic diagram of simulated SDL structure. (b) and (c) Are the calculated temperature distribution with pump spot diameter of 600 μm and 400 μm, respectively.

Table 2
Parameters for the Simulation of Temperature Distribution in SDL

Layer	RPG	DBR	AuIn	Cu-Sn	Diamond	Cu-Sn	AuIn	Heat sink
Thickness (μm)	1.46	3.72	1	0.1	1200	0.1	100	2500
Heat conductivity (W/mK)	32.5	32	162	61	1800	61	162	395

seen that there is no any bubble at the interface. In addition, this alloy also increases the wettability for the metallization of the diamond and enhances the interfacial bonding strength [22]. This might be the reason why the SDL bonded on the pre-metalized diamond has a lower thermal resistance.

According to the above discussion, it can be seen that the output power of SDL was affected significantly by the thermal management, and the performance of SDL was limited by the thermal rollover. The occurrence of thermal rollover is because the generated heat cannot be extracted out effectively. Enlarge the thermal dissipation area is the other approach to enhance emission power of SDL. Larger pump area means larger thermal dissipation area for SDL, and the thermal resistance will also be reduced [18], [20]. To study the heat dissipation in the active area of SDL, a simulation on the influence of pump spot sizes on the temperature of the gain area was performed. Fig. 6 shows the calculated temperature distribution of the SDL at dissipated power of 50 W with pump diameter of 400 μm and 600 μm. Since the temperature distribution seems to be almost rotationally symmetric, the cross-sections were shown. The simulation parameters used are list in Table 2, and the value selection of some parameters was according to Ref.20. As can be seen

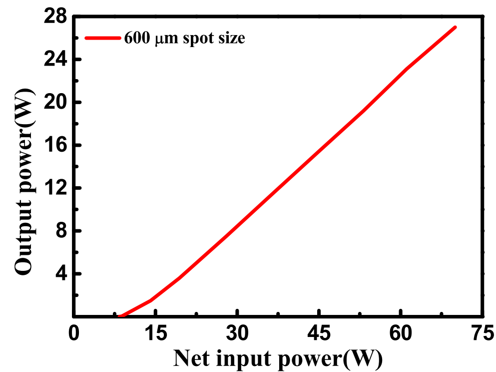

Fig. 7. Output power of SDL bonded on pre-metalized diamond with pump spot diameter of 600 μm.

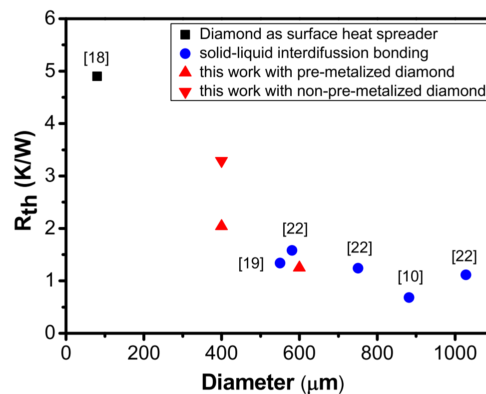

Fig. 8. Comparison of the thermal resistance Rth as a function of pump spot diameter with different packaging methods.

from Fig. 6(b), the maximum temperature at the active area of SDL for pump spot diameter of 600 μm is 68.2 °C, in contrast, it reaches 120 °C if the pump spot diameter shrinks to 400 μm from Fig. 6(c). It implies that expanding the pump spot size could decrease the temperature of the gain area, and hence postpone the occurrence of thermal rollover when increasing pump power, which means higher power could be realized.

We enlarge the pump spot diameter from 400 μm to 600 μm and perform on the SDL bonded on pre-metalized diamond which is the same one shown in Fig. 3. Fig. 7 shows the measured power performance. The TEC temperature is 12 °C. The threshold pump power is 8.4 W, corresponding to a threshold intensity of 2.97 kW/cm^2, which is almost same as the threshold intensity for pump spot diameter of 400 μm ($\sim$2.90 kW/cm^2) as shown in Fig. 3. The output power reaches 27 W and has no any thermal rollover at the net input power of 70 W, which is the maximum available net input power from our pump laser source. The maximum optical-to-optical efficiency of 46.5% was realized. Hence enlarging the pump spot size could indeed postpone the occurrence of thermal rollover and achieve higher output power. A similar measurement with Fig. 4 gets the thermal resistance for 600 μm pump spot size is $R_{th} = 1.25 \pm 0.21$ K/W. We compare the R_{th} results of SDL realized in this work with those achieved by other packaging methods at different values of pump parameters, as shown in Fig. 8. It can be seen the thermal resistance achieved by pre-metallized diamond is a little bit better than that of solid-liquid interdifussion at similar pump spot size of 600 μm, and it shows a tendency to continue improving for larger pump spot size, which presents a potential possibility to realize lower thermal resistance for SDL thermal management.

4. Conclusion

We demonstrated a pre-metalized process to reduce strongly the thermal resistance of a high-power SDL. This technological process makes a good bonding quality between SDL and diamond heat-spreader. The thermal resistance of SDL was improved, and the maximum output power is about twice of the SDL with non-metalized diamond. Finally, through the pre-metalized diamond and increasing the pump spot size up to 600 μm, the output power exceeding 27 W and a maximum optical-to-optical efficiency of 46.5% were realized.

References

[1] M. R. Johnson and N. Holonyak Jr., "Optically pumped thin-platelet semiconductor lasers," *J. Appl. Phys.*, vol. 39, no. 8, pp. 3977–3985, 1968.
[2] H. Le, S. Di Cecca, and A. Mooradian, "Scalable high-power optically pumped GaAs laser," *Appl. Phys. Lett.*, vol. 58, no. 18, pp. 1967–1969, 1991.
[3] S. Shu *et al.*, "Progress of optically pumped GaSb based semiconductor disk laser," *Opto-Electron. Adv.*, vol. 1, no. 2, pp. 17000301–17000309, 2018.
[4] M. Kuznetsov, F. Hakimi, R. Sprague, and A. Mooradian, "Design and characteristics of high-power (>0.5-W CW) diode-pumped vertical-external-cavity surface-emitting semiconductor lasers with circular TEM_{00} beams," *IEEE J. Sel. Topics Quantum Electron.*, vol. 5, no. 3, pp. 561–573, May/Jun. 1999.
[5] W. Jiang, S. Friberg, H. Iwamura, and Y. Yamamoto, "High powers and subpicosecond pulses from an external-cavity surface-emitting InGaAs/InP multiple quantum well laser," *Appl. Phys. Lett.*, vol. 58, no. 8, pp. 807–809, 1991.
[6] M. Kuznetsov, F. Hakimi, R. Sprague, and A. Mooradian, "High-power (>0.5-W CW) diode-pumped vertical-external-cavity surface-emitting semiconductor lasers with circular TEM_{00} beams," *IEEE Photon. Technol. Lett.*, vol. 9, no. 8, pp. 1063–1065, Aug. 1997.
[7] J. Sandusky and S. Brueck, "A CW external-cavity surface-emitting laser," *IEEE Photon. Technol. Lett.*, vol. 8, no. 3, pp. 313–315, Mar. 1996.
[8] T. Yao, "Thermal properties of AlAs/GaAs superlattices," *Appl. Phys. Lett.*, vol. 51, no. 22, pp. 1798–1800, 1987.
[9] A. R. Zakharian, J. Hader, J. V. Moloney, S. W. Koch, P. Brick, and S. Lutgen, "Experimental and theoretical analysis of optically pumped semiconductor disk lasers," *Appl. Phys. Lett.*, vol. 83, no. 7, pp. 1313–1315, 2003.
[10] B. Heinen *et al.*, "106 W continuous-wave output power from vertical-external-cavity surface-emitting laser," *Electron. Lett.*, vol. 48, no. 9, pp. 516–517, 2012.
[11] A. Chernikov *et al.*, "Heat management in high-power vertical-external-cavity surface-emitting lasers," *IEEE J. Sel. Topics Quantum Electron.*, vol. 17, no. 6, pp. 1772–1778, Nov./Dec. 2011.
[12] J. V. Moloney, J. Hader, and S. W. Koch, "Quantum design of semiconductor active materials: Laser and amplifier applications," *Laser Photon. Rev.*, vol. 1, pp. 24–43, 2007.
[13] D. Burns *et al.*, "Recent developments in high-power short-wave mid-infrared semiconductor disk lasers," *Proc. SPIE*, vol. 7193, 2009, Art. no. 719311.
[14] B. Rudin *et al.*, "Highly efficient optically pumped vertical-emitting semiconductor laser with more than 20 W average output power in a fundamental transverse mode," *Opt. Lett.*, vol. 33, no. 22, pp. 2719–2721, 2008.
[15] H. Hoff *et al.*, "Ohmic contacts to semiconducting diamond using a Ti/Pt/Au trilayer metallization scheme," *Diamond Rel. Mater.*, vol. 5, no. 12, pp. 1450–1456, 1996.
[16] A. Laurain, M. Myara, G. Beaudoin, I. Sagnes, and A. Garnache, "Multiwatt-power highly-coherent compact single-frequency tunable vertical-external-cavity-surface-emitting-semiconductor-laser," *Opt. Exp.*, vol. 18, no. 14, pp. 14627–14636, 2010.
[17] M. Mueller *et al.*, "Optically pumped semiconductor thin-disk laser with external cavity operating at 660 nm," *Proc. SPIE*, vol. 4649, pp. 265–272, 2002.
[18] S. Giet *et al.*, "Comparison of thermal management techniques for semiconductor disk lasers," *Proc. SPIE*, vol. 6871, 2008, Art. no. 687115.
[19] B. Heinen, F. Zhang, M. Sparenberg, B. Kunert, M. Koch, and W. Stolz, "On the measurement of the thermal resistance of vertical-external-cavity surface-emitting lasers (VECSELs)," *IEEE J. Quantum Electron.*, vol. 48, no. 7, pp. 934–940, Jul. 2012.
[20] B. Heinen, C. Möller, K. Jandieri, B. Kunert, M. Koch, and W. Stolz, "The thermal resistance of high-power semiconductor disk lasers," *IEEE J. Quantum Electron*, vol. 51, no. 5, 2015, Art. no. 2400109.
[21] J. Zhang, W. J. Lu, and W. Y. Yu, "Study on bonding mechanism of brazing of amorphous Cu-P filler metal," *Hot Work. Technol.*, vol. 37, no. 5, pp. 12–15, 2008.
[22] D. Z. Duan, B. Xiao, B. Wang, P. Han, W. J. Li, and S. W. Xia, "Microstructure and mechanical properties of pre-brazed diamond abrasive grains using Cu–Sn–Ti alloy," *Int. J. Refract. Met. Hard Mater.*, vol. 48, pp. 427–432, 2015.